Energy & Environmental Science

Cite this: DOI: 10.1039/c1ee01254a

www.rsc.org/ees

PAPER

An efficient DSSC based on ZnO nanowire photo-anodes and a new D-π-A organic dye

James S. Bendall,†*[a] Lioz Etgar,†[b] Swee Ching Tan,[a] Ning Cai,[c] Peng Wang,[c] Shaik M. Zakeeruddin,[b] Michael Grätzel[b] and Mark E. Welland[a]

Received 3rd March 2011, Accepted 6th May 2011
DOI: 10.1039/c1ee01254a

Zinc oxide-titanium dioxide core-shell nanowire dye-sensitised solar cells have been synthesised, making use of a recently developed organic dye and iodide-based electrolyte. We have been able to demonstrate a cell efficiency of 2.53% under AM1.5 for our system. Compared to other cells based on vertically aligned, hydrothermally grown ZnO nanowires, and systems of comparable architecture, our device demonstrates one of the highest cell efficiencies to date and is due to the precise control of the semiconductor's growth and the high performance of the incorporated dye. We have carried out complete morphological analysis and have been able to fully characterise the device.

Introduction

Since their invention in 1991, dye-sensitised solar cells have established themselves as a credible alternative to expensive silicon PVs.[1] This is due to the low cost and ease of manufacture. Over the past two decades, the cell's conversion efficiencies, lifetime and stability have all been improved.[2] The architecture of a typical traditional DSSC consists of a sandwich of conductive glass pieces, between which is a porous conductive titania film sensitised with dye for absorbing incident light, and a redox electrolyte to provide electron regeneration. The titania film acts as both a scaffold with a high surface-to-volume ratio for increased loading of the dye, and as a conductive pathway to remove the electrons donated by the dye molecules. The pathway for the generated electron through the titania film is *via* a hopping mechanism between the grain boundaries of the nanocrystals.[3] As such, a sintering procedure must be carried out on the TiO_2 film before dye loading in order to improve the nanoparticle-nanoparticle interface. However, this still means that charge carriers have to move across many particle boundaries. One-dimensional nanostructures should therefore improve charge carrier transportation by providing a facile direct electron pathway and lowering the diffusion resistance.[4] One-dimensional, epitaxially grown TiO_2 is possible to synthesise, but it is not a straightforward procedure.[5] A promising alternative is that of zinc oxide, which has very similar electronic structure to TiO_2 but can be grown under much milder, more controllable conditions.[6] Furthermore, ZnO has been shown to have higher electron mobility than TiO_2, potentially allowing for faster kinetics and fewer recombinations.[7] Nanowires (NWs) of ZnO have been

[a]*Nanoscience Centre, University of Cambridge, 11 JJ Thomson Ave, Cambridge, CB3 0FF, UK. E-mail: jsb53@cam.ac.uk*
[b]*Laboratory for Photonics and Interfaces, Swiss Federal Institute of Technology, CH 1015 Lausanne, Switzerland*
[c]*State Key Laboratory of Polymer Physics and Chemistry, Changchun Institute of Applied Chemistry, Chinese Academy of Sciences, Changchun, 130022, China*
† Both authors contributed equally to this work.

Broader context

Global warming, dwindling carbon-based supplies, high fuel prices and rising population levels have recently focussed considerable interest in the production of energy from alternative sources. Photovoltaic (PV) devices, which convert the sun's energy into electrical current, are already widely used, though silicon-based devices currently dominate the field. These devices are very stable and show a relatively high energy conversion efficiency but are expensive to produce. Recently, devices such as dye-sensitized solar cells (DSSC) have generated great interest due to their inexpensive manufacture and favourable architecture. Traditionally these have been made with TiO_2 nanoporous layers but recently other metal oxides such as ZnO have been investigated. One challenge is to improve the performance of such devices through careful engineering of the active layers and through the design and synthesis of novel sensitizers. In this paper we report a highly efficient ZnO nanowire-based device, taking advantage of the highly controllable growth of the photoanode and utilizing a new D-π-A organic dye, the first time such a dye has been demonstrated in a ZnO-based dye-sensitized solar cell.

extensively demonstrated to grow under numerous conditions including hydrothermal synthesis,[8] Chemical Vapour Deposition (CVD)[9] or electrochemical deposition.[10] Of these, the aqueous methods allow growth to occur at lower temperatures, decreasing the cost of production and enabling non-rigid substrates to be used. For all their promise, however, ZnO nanowire-based DSSCs have not performed as well as their TiO_2-based cousins. A number of factors are to blame for this. High efficiencies require high dye-loading. Typically TiO_2-based DSSCs use semiconducting layers of around 20 μm thick to ensure a high amount of dye can be incorporated into the active layer. Growing ZnO NWs of comparable length and internal surface area under hydrothermal conditions is not trivial due to competing homogeneous and heterogeneous nucleation processes. Furthermore, the surface of ZnO is known to be chemically unstable and to contain surface trap states. For many of the commercially available Ru-based dyes, aggregates rather than monolayers are seen to form on the nanowire surface.[11] Recently, much research has been devoted to solving many of these issues in order to improve ZnO Nanowire-based DSSC device performance – increasing the internal surface area through the growth of longer NWs, designing core-shell structures to suppress electron-hole recombination[12,13] or improving and enhancing oxide-dye coupling.

Nevertheless, the highest efficiencies of DSSCs constructed using many of these aligned ZnO NW arrays are less than 2%.[14] It has long been known that ZnO NW-based DSSCs have suffered from low efficiencies through a combination of low levels of dye adsorption (due to the thinness of the active layer), unstable surface chemistry, defect states and incompatible ZnO-dye interaction.[15] We have addressed these major issues through careful engineering and optimisation of the photoanode and through the use of a new D-π-A organic dye in order to improve device efficiencies.

In this article we describe a solar cell constructed using a newly developed organic dye (C220) with high molar extinction coefficient ε of 5.5×10^4 M^{-1} cm^{-1} at 555 nm. The energy offset of the LUMO (−3.42 eV) of the C220 dye molecule with respect to the ZnO conduction band edge (∼−4.0 eV)[16] provides the driving force for charge injection.[17] The molecular structure of the **C220** dye is presented in Fig. 1, The 4,4′-didodecyl-4*H*-cyclopenta[2,1-*b*:3,4-*b*′]dithiophene (CPDT) segment is used as the spacer between the donor and the acceptor group (**D-π-A**) of this organic sensitizer. This is the first time such dye has been reported in liquid electrolyte solar cells and in combination with a ZnO active layer, which we have also developed to have a high surface area and good electron transport capabilities. Our best device performance shows an open-circuit voltage (V_{oc}) of 819.6 mV, a short circuit current density (Jsc) of 5.08 mA cm^{-2} and a fill factor of 60.6% with power conversion efficiency of 2.53% under 1.5AM, which is one of the best device performances reported so far in the literature for vertically aligned ZnO nanowires. This performance was achieved using core shell NWs of ZnO/TiO_2.

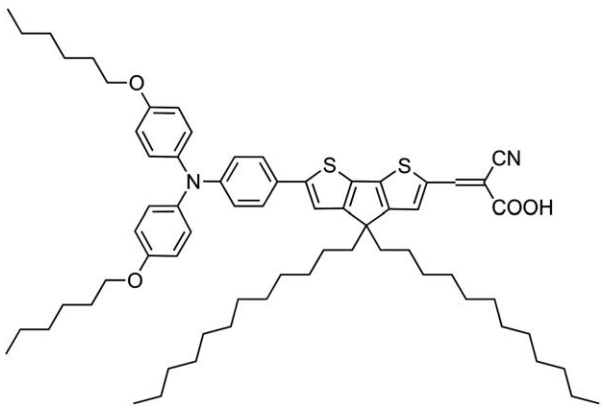

Fig. 1 The molecular structure of C220.

Experimental

Materials

All solvent and reagents were of puriss grade quality and were used as received. Guanidium thiocyanate (GuNCS) was purchased from Fluka. Zinc nitrate (99.999%) and poly(ethyleneimine) (end capped, M_W ∼800 g mol^{-1}) were purchased from Sigma-Aldrich. Hexamethylene tetramine (99 + %) was purchased from Alfa Aesar. 1,3-dimethylimidazolium iodide (DMII) was prepared accordingly to a reported procedure[18] and the purity was confirmed by ^{1}H NMR analysis.

ZnO nanowires (NWs) growth and characterisation

ZnO Nanowires were grown on FTO-coated glass (Solaronix FTO22-15) *via* a hydrothermal route. The substrate was cleaned in acetone, isopropanol and water and dried under a stream of nitrogen. A thin layer of zinc metal was sputtered onto the FTO surface through a shadow mask with a hole of 6mm diameter, which defines the active area of the cell. The sputtered zinc layer acted as both a seed layer and a blocking layer and was placed within a pre-heated (1 h at 92 °C) growth solution containing 74mM zinc nitrate, 50 mM hexamethylene tetramine (HMT) and 4.5 mM poly(ethyleneimine) (end capped, M_W ∼800 g mol^{-1}). The substrate was held at 92 °C for 3 h before being placed within a second pre-heated reaction vessel containing identical precursors. To achieve 10 μm NWs, this step was repeated a further 8 times. Post-growth, the active areas were washed well in deionised water and dried. Morphological characterisation was carried out in a FEG-SEM (Carl Zeiss Leo 1530VP with Gemini column) operated at 10keV. Raman spectroscopy was performed on a Renishaw spectrometer through a 50x objective and in the backscattering geometry. A green excitation laser at 514.5 nm was used as the excitation source. TEM was carried out at 200 keV in a Philips Tecnai 20 HRTEM. TEM samples were prepared by removing the nanowires from the substrate using a blading technique, dispersing them in ethanol using sonication and dropping them onto a holey carbon TEM grid.

Core shell ZnO/TiO_2 (NWs) growth

TiO_2 shells were grown on the NW arrays using a modified Beneq ALD system operated at 10^{-6} mbar. Titania was deposited on the NW from titanium tetrachloride and distilled water sources at 250 °C using 500 ms pulse, 300 ms purge cycles. The average growth rate was ∼0.5 Å per cycle.

Solar cell fabrication

The dye-sensitized solar cell was assembled by sandwiching the dye-sensitized ZnO–NWs semiconductor component with the Pt-coated FTO cathode using a piece of hot melt Surlyn (25 μm thick) as a spacer. The ZnO NWs film was stained by immersing it into a dye solution (C220) in a mixture of acetonitrile and ter-butanol (volume ratio 1 : 1) for 4 h.[17] Several dipping times were tried; the optimal loading time (4 h) was found by measuring the photovoltaic performance of each immersion time. Finally the internal space of the DSC was filled with a redox electrolyte consisting of 1.0 M DMII, 50 mM LiI, 30 mM I_2, 0.5 M TBP, and 0.1 M GNCS in the mixture of acetonitrile and valeronitrile (v/v, 85/15).

Photovoltaic characterization

Photovoltaic measurements employed an AM 1.5 solar simulator equipped with a 450W xenon lamp (Model No. 81172, Oriel). Its output was calibrated to 100 MW cm^{-2} by using a reference Si photodiode equipped with an IR-cutoff filter (KG-3, Schott) in order to reduce the mismatch between the simulated light and AM 1.5 (in the region of 350–750 nm) to less than 2% with measurements verified at two PV calibration laboratories [ISE (Germany), NREL (USA)]. *I–V* curves were obtained by applying an external bias to the cell and measuring the generated photocurrent with a Keithley model 2400 digital source meter. The voltage step and delay time of the photocurrent were 10 mV and 40 ms, respectively. The photovoltaic measurements were taken by using a metal mask with an aperture area of 0.159 cm^2. A similar data acquisition system was used to determine the monochromatic incident photon-to-electric current conversion efficiency. Under full computer control, light from a 300 W xenon lamp (ILC Technology, USA) was focused through a Gemini-180 double monochromator (Jobin Yvon Ltd., U.K.) onto the photovoltaic cell under test. The monochromator was incremented through the visible spectrum to generate the IPCE (λ) as defined by IPCE (λ) = 12400(Jsc/λφ), where λ is the wavelength, Jsc is short-circuit photocurrent density (mA cm^{-2}), and φ is the incident radiative flux (mW cm^{-2}).

Results and discussion

ZnO NWs growth mechanism and characterisation

Fig. 2 shows the nanostructures grown on the FTO electrode in the area covered with a sputtered Zn film. The crystals are mainly hexagonal in shape and have a range of diameters, mainly clustered at 50 nm ±30nm. Some nanowires are slightly longer and thicker than the majority. Side-view imaging shows that the wires are vertically aligned with respect to the substrate surface with a length of 10 μm for a 27 h growth time. Extending or decreasing the total growth time led to longer or shorter NW electrodes, respectively. The crystallisation of ZnO using the hydrothermal method takes place *via* a number of chemical reactions in the growth solution.[19] The major ones are outlined below. Above 60 °C, the HMT solution undergoes the following reactions:

$$C_6H_{12}N_4 + 6H_2O \rightarrow 6HCHO + 4NH_3 \quad (1)$$

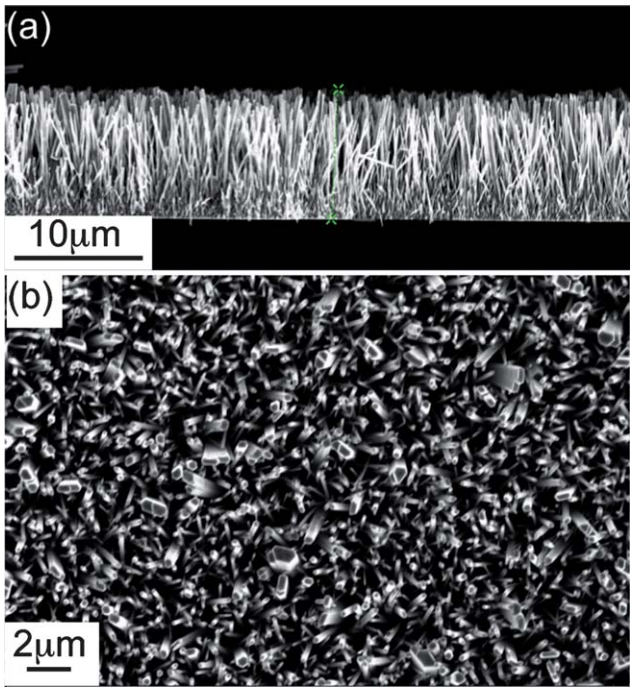

Fig. 2 SEM imaging of as-made vertically aligned 10 μm long ZnO nanowires synthesized on FTO-coated glass *via* the hydrothermal method at 92 °C for a total growth time of 27 h. (a) Side view imaging; (b) top view imaging.

$$NH_3 + H_2O \leftrightarrow NH_4^+ + OH^- \quad (2)$$

This allows the following chemical reactions to occur, ultimately forming ZnO:

$$Zn^{2+}_{(aq)} + 2OH^- \leftrightarrow Zn(OH)_2 \leftrightarrow ZnO(s) + H_2O \quad (3)$$

Additional chemicals introduced into the growth solution can often alter the morphology of the ZnO either through adsorption onto specific crystal faces, which can prevent growth in certain directions, or through alterations in growth rates.[19,20] Polyethylene imine has been shown to preferentially bind to the six non-polar prismatic $\{10\bar{1}0\}$ crystal faces, thereby promoting growth along the c-direction of the crystal and preventing lateral expansion of the nanowires.[21] Initial growth takes place on the nuclei of the seed layer that, in our case, is a highly uniform sputtered Zn film deposited onto the FTO layer. Within the hot growth solution rapid oxidation of the sputtered layer can take place to produce a ZnO surface. The freshly prepared ZnO surface comprises of ZnO grains (approx. 20–30 nm in size), which act as nucleation sites for the growth of nanocrystals.[22] Pre-heating the solution prior to introduction of the seed layer allows the rapid homogeneous nucleation process to proceed, decreasing the supersaturation level of the precursors and for the ZnO formation to enter into an equilibrium condition. Once the substrate has been introduced into the pre-heated solution, and rapidly oxidised, crystal growth can favourably occur on the exposed ZnO grains.[23] In this way, we were able to produce long, vertically aligned ZnO nanowires up to 10 μm long over a period

of a 27 h growth time, thereby increasing the surface area available for dye adsorption.

Photovoltaic performance of ZnO NWs

Fig. 3 illustrates the structure of the NWs DSSC using the ZnO NWs. The device is illuminated from the transport electrode, in the same fashion as that of many other 1-D semiconducting nanoarchitecture-based DSSCs. The ZnO NWs are grown vertically on FTO-coated glass substrates (Fig. 2).

The ZnO NWs film was stained by immersing it into a dye solution of C220 in a mixture of acetonitrile and ter-butanol (volume ratio 1 : 1) for 4 h.[17] The sensitized ZnO electrode was assembled with a thermally platinized FTO counter electrode and surlyn hot melt as a spacer. The internal space was filled with a redox electrolyte consists of 1.0 M DMII, 50 mM LiI, 30 mM I_2, 0.5 M TBP, and 0.1 M GNCS in the mixture of acetonitrile and valeronitrile (v/v, 85/15). The overall energy conversion efficiency of 1.25% (*V*oc, 524.1 mV; *J*sc, 5.49 mA $cm^{-1}2$; *ff*, 0.43) was measured under irradiation of 100 mW cm^{-2} AM 1.5G sunlight. The photocurrent-voltage characteristics of the ZnO NWs DSC is shown in Fig. 4a. The best photovoltaic performance was obtained using 10 μm thickness of ZnO NWs film.

The incident photon to current conversion efficiency (IPCE), external quantum efficiency, specifies the ratio of extracted electrons to incident photons at a given wavelength. The IPCE spectrum (Fig. 4b) is plotted as a function of wavelength of the light. The ZnO NWs cell shows a good response at 470 nm wavelength the IPCE is reaching its maximum of 69%, while at 600 nm wavelength the IPCE is 15%.

Integration of the IPCE spectrum over the AM1.5 solar emission yields a photocurrent density of 6.67 mA cm^{-2} in good agreement with the measured spectrum showing that any mismatch between the true AM 1.5 emission and that of the solar simulator is small. Our reported efficiency for bare ZnO NWs of 10 μm length compares favourably with current literature device performances.[14,21]

Improvements in device performance for ZnO NW-based photovoltaic devices have often been observed when the NWs have been coated with thin layers of semiconducting or insulating materials.[24] These have included MgO, Al_2O_3 and ZrO_2. The purpose of these shells is to provide a more stable binding site for dye absorption and suppress carrier recombination.[12] Core-shell structures of ZnO–TiO_2 have been synthesised using ALD methods, allowing precise control of the shell thickness coating the NW surface.

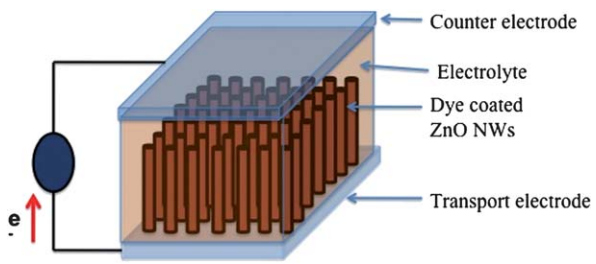

Fig. 3 A schematic showing the structure of the NW-based DSSC.

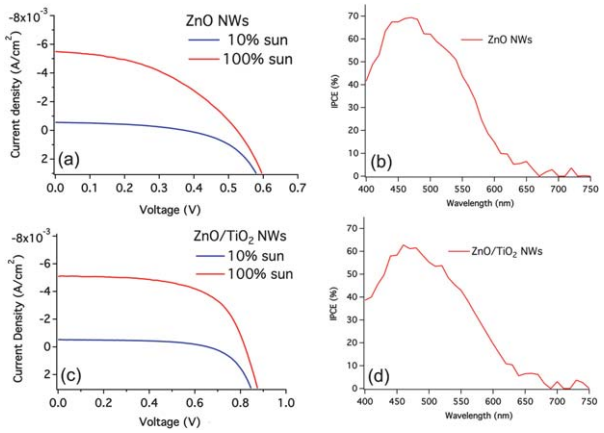

Fig. 4 (a) Photocurrent-voltage characteristics and (b) IPCE spectrum of as-made 10 μm length ZnO NW C220 DSSC. (c) photocurrent-voltage characteristics and (d) IPCE spectrum of core-shell ZnO–TiO_2 C220 NW-based DSSCs. The length of the ZnO NWs is 10 μm, the thickness of the shell is 20 nm.

Core shell ZnO/TiO_2 NWs characterisation

Fig. 5 outlines the characterisation of the NW arrays following TiO_2 treatment in the ALD. SEM imaging (Fig. 5a) shows that the highly porous nature of the nanowire film has been preserved

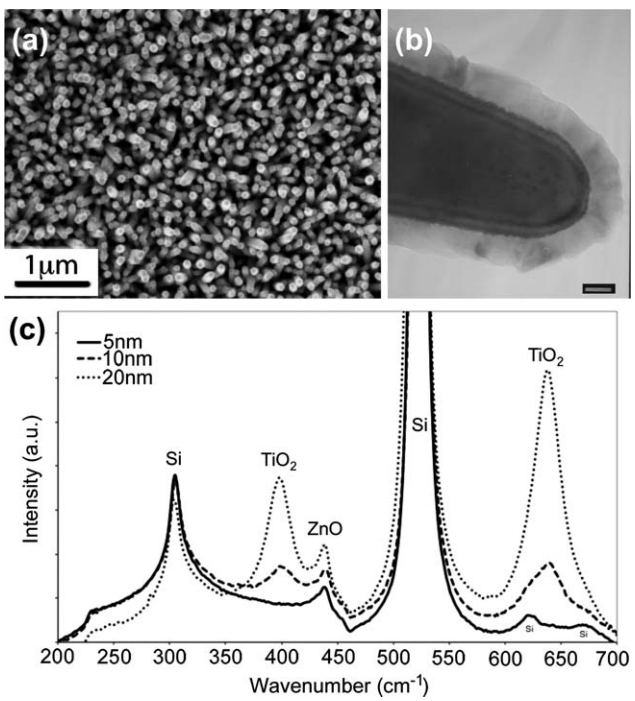

Fig. 5 Characterisation of the ZnO–TiO_2 core-shell structures and arrays synthesized *via* the hydrothermal-ALD method. (a) Top-view SEM imaging of highly porous arrays of ZnO–TiO_2 core-shell NWs, with 10 μm long ZnO NWs and 20 nm thick TiO_2 coating. (b) TEM imaging of the tip of a single TiO_2-coated (20 nm thick) ZnO NW. Scale bar corresponds to 20 nm. (c) Raman spectroscopic characterization of different TiO_2 shell thicknesses on ZnO NW arrays (grown on Si wafer). Shell thicknesses were measured as 5 nm (solid line), 10 nm (dashed line) and 20 nm (dotted line).

after titania deposition. From TEM characterisation (Fig. 5b) we can see that a thin shell, the thickness of which is measured as 20 nm, covers the individual nanowires. Raman spectroscopy (Fig. 5c) of the core-shell structures shows a number of peaks corresponding to ZnO and TiO_2 vibration modes. Normalisation of the peaks to the Si peak at 520.5 cm^{-1} allows the comparison of the ZnO peak (at ~430 cm^{-1}) to the TiO_2 peak. Vibrations which are due to the TiO_2 shell are observed at ~197 cm^{-1} and ~635 cm^{-1}, and can be assigned to the B_{1g} and E_g active modes, respectively, for anatase TiO_2.[25] As the shell thickness increases, the intensities of the TiO_2 peaks increase with respect to the ZnO peak. No discernable peaks are observed for the 5 nm shell sample. This is in agreement with the observation that, below 5 nm, the layer is amorphous.[12]

The core-shell structures of ZnO–TiO_2 have been synthesised using ALD, through a pulse/purge combination of $TiCl_4$ and H_2O, and conformal coatings of TiO_2 can be achieved; longer pulse times of titanium chloride ensure that precursors can diffuse into the highly porous ZnO NW array. Shell thicknesses ranging from 5 nm to 40 nm were tested in devices for ZnO films of 1μm thickness (Fig. 6). The highest efficiencies were seen for cells with 20 nm TiO_2 shell deposited on the ZnO. Above this optimum thickness, SEM images suggested that the dye was unable to penetrate within the nanowire array due to the tight spacing between the NWs.

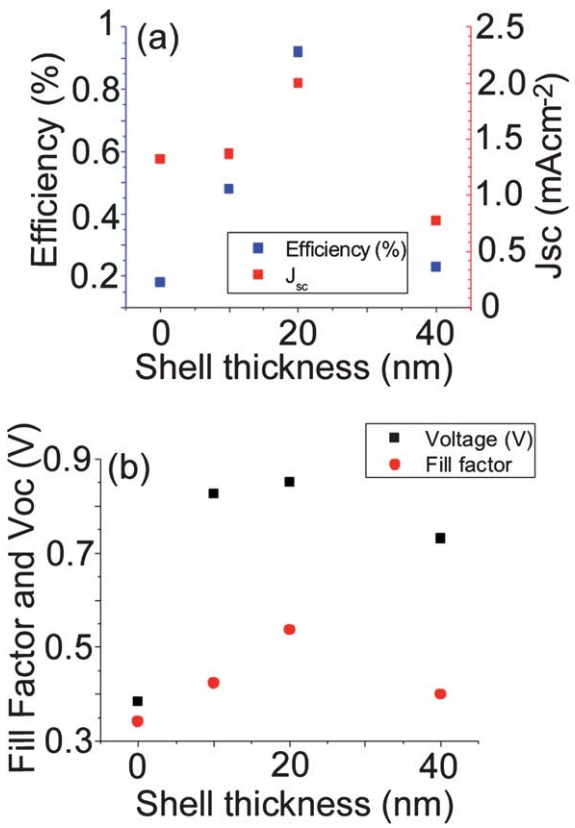

Fig. 6 C220 DSSC device performance characterization for core-shell ZnO–TiO_2 photoanodes of different TiO_2 shell thicknesses on 1 μm long ZnO NWs. (a) efficiency (%) (blue squares) and Jsc (mA cm^{-2}) (red squares); (b) voltage (V) (black squares) and fill factor (red spots). Optimal performance was observed for shells of 20 nm thickness.

Table 1 Comparison of the photovoltaic properties of bare ZnO NWs and ZnO/TiO_2 core shell NWs based DSSCs

	Voc (mV)	Jsc (mA cm^{-2})	FF	Efficiency at 1.5AM
ZnO NWs	524.1	5.49	43	1.25
ZnO/TiO_2 NWs	819.6	5.08	60.6	2.53

Photovoltaic performance of ZnO/TiO_2 NWs

As shown in Fig. 6, TiO_2 shell thickness of 20 nm gave the best photovoltaic performance using 1μm thickness of ZnO/TiO_2 core shell film. Using this finding we made 10μm long core ZnO NWs covered with 20nm TiO_2 shell creating ~10μm thickness ZnO/TiO_2 film. Table 1 summarizes the photovoltaic performance obtained from the bare ZnO NWs cell and the ZnO/TiO_2 cell. The photocurrent-voltage characteristic of the ZnO/TiO_2 core shell structure is shown in Fig. 4c. The cell shows an open-circuit voltage (Voc) of 819.6 mV, a short circuit current density (Jsc) of 5.08mA cm^{-2} and a fill factor of 60.6% with power conversion efficiency of 2.53% under 1.5AM. The fill factor and the Voc improve significantly with the 20nm TiO_2 shell compared to the bare ZnO NWs. The TiO_2 shells suppress recombination, by introducing an energy barrier that increases the physical separation between photoinjected electrons and the oxidized redox species in the electrolyte.[12] The full- scale semilogarithmic plots in Fig. 7 show that the dark current of the bare ZnO NWs DSSC is higher than the dark current of the ZnO/TiO_2 NWs DSSC. A smaller dark current suggest a lower rate of recombination which results an increasing of the Voc and the fill factor, which agrees well with our results.

The IPCE spectrum of the cell is shown in Fig. 4d. At 460nm wavelength, the IPCE reaches its maximum of 63% while at 600nm wavelength the IPCE is 20%. A different shape of the IPCE can be seen for the core shell NWs compared to the bare ZnO NWs. The TiO_2 shell provides a more stable binding site for the dye absorption. As a result, at higher wavelengths starting at 570 nm, the IPCE of the core shell NWs is higher than the IPCE of the bare ZnO NWs. Integration of the IPCE spectrum over the AM1.5 solar emission yields a photocurrent density of 6.23 mA cm^{-2} in good agreement with the measured spectrum showing that any mismatch between the true AM 1.5 emission and that of the solar simulator is small.

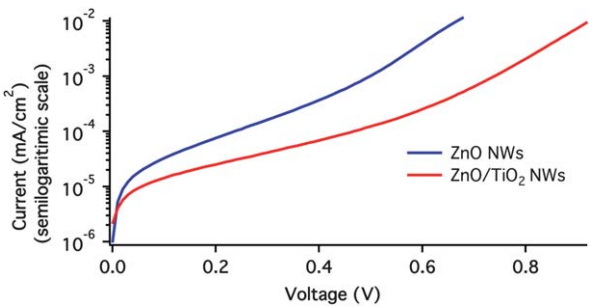

Fig. 7 Full-scale semilogarithmic current–voltage plots of ZnO NW DSSC and ZnO–TiO_2 DSSC, taken in the dark. Both DSSCs were constructed with 10 μm long ZnO NWs; for the core-shell device, the optimal TiO_2 thickness of 20 nm was used.

Conclusions

We have demonstrated a high performance ZnO NWs DSSC based on the favorable combination of a highly reproducible, carefully engineered, high surface-to-volume ratio photoanode and a newly developed organic dye. The PV performance of the ZnO NWs was further improved and enhanced by making a core shell of highly crystalline TiO_2 on top of ZnO NWs through ALD-based methods. The shells were tuned to the optimum thickness for enhanced cell performance and were highly conformable down the length of the NW. They contributed to an increase in the open circuit voltage and the fill factor and allowed PCE values to reach as high as 2.5% under 100 mW cm^{-2}, AM1.5G sunlight.

Acknowledgements

This research was funded by the European Community's Seventh Framework Programme (FP7/2007-2013) under grant agreement n° 227057, Project "INNOVASOL". L.E. acknowledges the Marie Curie Actions—Intra-European Fellowships (FP7-PEOPLE-2009-IEF) under grant agreement n° 252228, project "Excitonic Solar Cell". N.C. and P.W. thank the National 973 Program (No. 2007CB936702 and No. 2011CBA00702) for financial support. The authors thank Dr Suman-Lata Sahonta for HRTEM characterization.

References

1 B. O'Regan and M. Gratzel, *Nature*, 1991, **353**, 737.
2 M. K. Nazeeruddin, A. Kay, I. Rodicio, R. Humphry-Baker, E. Mueller, P. Liska, N. Vlachopoulos and M. Graetzel, Conversion of light to electricity by cis-X2bis(2,2′-bipyridyl-4,4′-dicarboxylate)ruthenium(II) charge-transfer sensitizers (X = Cl-, Br-, I-, CN-, and SCN-) on nanocrystalline titanium dioxide electrodes, *J. Am. Chem. Soc.*, 1993, **115**(14), 6382–6390.
3 K. D. Benkstein, N. Kopidakis, J. van de Lagemaat and A. J. Frank, Influence of the Percolation Network Geometry on Electron Transport in Dye-Sensitized Titanium Dioxide Solar Cells, *J. Phys. Chem. B*, 2003, **107**(31), 7759–7767.
4 I. Gonzalez-Valls and M. Lira-Cantu, Vertically-aligned nanostructures of ZnO for excitonic solar cells: a review, *Energy Environ. Sci.*, 2009, **2**(1), 19–34.
5 X. Feng, K. Shankar, O. K. Varghese, M. Paulose, T. J. Latempa and C. A. Grimes, Vertically Aligned Single Crystal TiO2 Nanowire Arrays Grown Directly on Transparent Conducting Oxide Coated Glass: Synthesis Details and Applications, *Nano Lett.*, 2008, **8**(11), 3781–3786.
6 L. Vayssieres, Growth of arrayed nanorods and nanowires of ZnO from aqueous solutions, *Adv. Mater.*, 2003, **15**(5), 464–466.
7 M. Quintana, T. Edvinsson, A. Hagfeldt and G. Boschloo, Comparison of Dye-Sensitized ZnO and TiO2 Solar Cells: Studies of Charge Transport and Carrier Lifetime, *J. Phys. Chem. C*, 2007, **111**(2), 1035–1041.
8 L. E. Greene, B. D. Yuhas, M. Law, D. Zitoun and P. Yang, Solution-Grown Zinc Oxide Nanowires, *Inorg. Chem.*, 2006, **45**(19), 7535–7543.
9 J. I. Sohn, S. S. Choi, S. M. Morris, J. S. Bendall, H. J. Coles, W.-K. Hong, G. Jo, T. Lee and M. E. Welland, Novel Nonvolatile Memory with Multibit Storage Based on a ZnO Nanowire Transistor, *Nano Lett.*, 2010, **10**(11), 4316–4320.
10 J. Elias; C. Levy-Clement; M. Bechelany; J. Michler; G. Y. Wang; Z. Wang; L. Philippe, Hollow Urchin-like ZnO thin Films by Electrochemical Deposition. *Advanced Materials* 22((14)), p. 1607.
11 T. P. Chou, Q. Zhang and G. Cao, Effects of Dye Loading Conditions on the Energy Conversion Efficiency of ZnO and TiO2 Dye-Sensitized Solar Cells, *J. Phys. Chem. C*, 2007, **111**(50), 18804–18811.
12 M. Law, L. E. Greene, A. Radenovic, T. Kuykendall, J. Liphardt and P. Yang, ZnO-Al2O3 and ZnO-TiO2 Core-Shell Nanowire Dye-Sensitized Solar Cells, *J. Phys. Chem. B*, 2006, **110**(45), 22652–22663.
13 S. H. Kang, J.-Y. Kim, Y. Kim, H. S. Kim and E. Sung Y-, Surface Modification of Stretched TiO2 Nanotubes for Solid-State Dye-Sensitized Solar Cells, *J. Phys. Chem. C*, 2007, **111**, 9614–9623.
14 S. Yodyingyong, Q. Zhang, K. Park, C. S. Dandeneau, X. Zhou, D. Triampo and G. Cao, ZnO nanoparticles and nanowire array hybrid photoanodes for dye-sensitized solar cells, *Appl. Phys. Lett.*, 2010, **96**(7), 073115.
15 Q. Zhang, C. S. Dandeneau, X. Zhou and G. Cao, ZnO Nanostructures for Dye-Sensitized Solar Cells, *Adv. Mater.*, 2009, **21**, 4087–4108.
16 M. Grätzel; Photoelectrochemical Cells, *Nature* 414 pp. 338–344.
17 N. Cai, S.-J. Moon, L. Cevey-Ha, T. Moehl, R. Humphry-Baker, P. Wang, S. M. Zakeeruddin and M. Gratzel, An Organic D-π-A Dye for Record Efficiency Solid-State Sensitized Heterojunction Solar Cells, *Nano Lett.*, 2011, DOI: 10.1021/nl104034e, *A*SAP.
18 P. Bonhote, A.-P. Dias, N. Papageorgiou, K. Kalyanasundaram and M. Gratzel, Hydrophobic, Highly Conductive Ambient-Temperature Molten Salts,Â†, *Inorg. Chem.*, 1996, **35**(5), 1168–1178.
19 J. S. Bendall, G. Visimberga, M. Szachowicz, N. O. V. Plank, S. Romanov, C. M. Sotomayor-Torres and M. E. Welland, An investigation into the growth conditions and defect states of laminar ZnO nanostructures, *J. Mater. Chem.*, 2008, **18**(43), 5259–5266.
20 Z. R. R. Tian, J. A. Voigt, J. Liu, B. McKenzie, M. J. McDermott, M. A. Rodriguez, H. Konishi and H. F. Xu, Complex and oriented ZnO nanostructures, *Nat. Mater.*, 2003, **2**(12), 821–826.
21 C. Xu, P. Shin, L. Cao and D. Gao, Preferential Growth of Long ZnO Nanowire Array and Its Application in Dye-Sensitized Solar Cells, *J. Phys. Chem. C*, 2009, **114**(1), 125–129.
22 J. S. Bendall and S. C. Tan, Investigating the Hydrothermal Growth of Zinc Oxide Nanostructures Through Seed Layer Control, *Zeitschrift für Physikalische Chemie*, 2011, **225**(2011), 10.
23 N. O. V. Plank, M. E. Welland, J. L. MacManus-Driscoll and L. Schmidt-Mende, The backing layer dependence of open circuit voltage in ZnO/polymer composite solar cells, *Thin Solid Films*, 2008, **516**(20), 7218–7222.
24 (*a*) N. O. V. Plank, H. J. Snaith, C. Ducati, J. S. Bendall, L. Schmidt-Mende and M. E. Welland, A simple low temperature synthesis route for ZnO–MgO core-shell nanowires, *Nanotechnology*, 2008, **19**(46); (*b*) N. O. V. Plank, I. Howard, A. Rao, M. W. B. Wilson, C. Ducati, R. S. Mane, J. S. Bendall, R. R. M. Louca, N. C. Greenham, H. Miura, R. H. Friend, H. J. Snaith and M. E. Welland, Efficient ZnO Nanowire Solid-State Dye-Sensitized Solar Cells Using Organic Dyes and Core-shell Nanostructures, *J. Phys. Chem. C*, 2009, **113**(43), 18515–18522.
25 H. L. Ma, J. Y. Yang, Y. Dai, Y. B. Zhang, B. Lu and G. H. Ma, Raman study of phase transformation of TiO2 rutile single crystal irradiated by infrared femtosecond laser, *Appl. Surf. Sci.*, 2007, **253**(18), 7497–7500.

